ELSEVIER

Contents lists available at ScienceDirect

Chemical Geology

journal homepage: www.elsevier.com/locate/chemgeo





Intramolecular hydrogen isotope exchange inside silicate melts – The effect of deuterium concentration

Nico Kueter^{a,b,*}, George D. Cody^b, Dionysis I. Foustoukos^b, Bjorn O. Mysen^b

- a Geological Institute, ETH Zürich, Sonnegestrasse 5, Zurich, Switzerland
- ^b Earth and Planets Laboratory, Carnegie Institution of Washington, 5241 Broad Branch Road NW, Washington DC 20015, USA

ARTICLE INFO

Editor: S Aulbach

Keywords: Silicate melt Deep water cycle Volatiles Hydrogen isotopes NMR spectroscopy

ABSTRACT

Tracing the deep geological water cycle requires knowledge of the hydrogen isotope systematics between and within hydrous materials. For quenched hydrous alkali-silicate melts, hydrogen NMR reveals a distinct heterogeneity in the distribution of stable hydrogen isotopes (D, H) within the silicate tetrahedral network, where deuterons concentrate strongly in network regions that are associated with alkali cations. Previous hydrogen NMR studies performed in the sodium tetrasilicate system (Na₂O x 4SiO₂, NS4) with a 1:1 D₂O/H₂O ratio showed on average 1300 % deuterium enrichment in the alkali-associated network, but the effect on varying bulk D_2O / H₂O ratios on this intramolecular isotope effect remained unconstrained. Experiments in the hydrous sodium tetrasilicate system with 8 wt% bulk water and varying bulk D_2O/H_2O ratios were performed at 1400 $^{\circ}C$ and 1.5 GPa. It is found that both hydrogen isotopes preferably partition into the silicate network that is associated with alkali ions. The partitioning is always stronger for the deuterated than for the protonated hydrous species. The relative enrichment of deuterium over protium in the alkali-associated network, i.e., the intramolecular isotope effect, correlates positively with the D₂O/H₂O bulk ratio of the hydrous NS4 system. Modeled for natural deuterium abundance (D/H near 1.56×10^{-4}), a 1.4-fold (c. 340 %) deuterium enrichment in the alkaliassociated silicate network is predicted. The partitioning model further predicts a positive correlation between the bulk water content of the silicate melt and the intramolecular deuterium partitioning into the alkaliassociated silicate network. Such heterogeneities may explain the magnitude and direction of hydrogen isotope fractionation in hydrous silicate melts coexisting with silicate-saturated fluids. As such, this intramolecular isotope effect appears to be an effective mechanism for deuterium separation, particularly in hydrous magmatic settings, such as subduction zones.

1. Introduction

The direction of hydrogen isotope fractionation in metamorphic and magmatic devolatilization reactions points towards a relative enrichment of deuterium into the fluid phase (Chacko et al., 2001; Shaw et al., 2008; Suzuoki and Epstein, 1976; Vennemann and ONeil, 1996). As a consequence of the geological deep water cycle, this nearly unidirectional hydrogen isotope fraction trend might produce deuterium-depleted restitic materials recycling into the mantle over geological time scales while creating ascending deuterium-rich fluids which contribute to the ever-increasing D/H ratio of Earth's oceans (Kurokawa et al., 2018; Lecuyer et al., 2020; Pope et al., 2012; Shaw et al., 2008). While this model is based on the general knowledge of hydrogen isotope fractionation behavior from experiments and natural observation, exact

hydrogen isotope fractionation mechanisms under the more extreme conditions of the Earth's interior remain insufficiently constrained.

Few existing experimental studies performed in the silicate melt – fluid systems (e.g., gas, vapor, silicate saturated fluids) reveal significant differences in the magnitude of hydrogen isotope fractionation (Dalou et al., 2015; Dobson et al., 1989; Mysen, 2013a; Mysen, 2013b; Pineau et al., 1998; Richet et al., 1986). Fractionation experiments performed in-situ in the Na-(Al)-Si-D₂O-H₂O system, while the sample was at high temperature and pressure in hydrothermal diamond anvil cells (HDAC), resulted in pronounced deuterium enrichment in the fluid phase (Dalou et al., 2015; Mysen, 2013a; Mysen, 2013b). At the same time, ¹H and ²H magic angle spinning (MAS) nuclear magnetic resonance (NMR) studies of samples quenched from high temperature at high pressure revealed intramolecular isotope fractionation inside alkali silicate glasses (Li, Na,

^{*} Corresponding author at: Geological Institute, ETH Zürich, Sonneggstrasse 5, Zurich, Switzerland. E-mail address: nico.kueter@erdw.ethz.ch (N. Kueter).

K) that might be linked to the enhanced isotopic fractionation observed in the fluid-melt system (Le Losq et al., 2016; Wang et al., 2015).

In a recent study, we investigated this intramolecular hydrogen isotope effect for the sodium tetrasilicate system (NS4, Na₂O·4SiO₂) with respect to variations in main experimental parameters, i.e., pressure, temperature, quench rate, and water content (Kueter et al., 2021). We observed great differences in the reactive behavior of the isotope-substituted hydrous species dissolved in the melt (Si-OX, X_2O_m , where X = H, D), and generally, there were high deuterium concentrations near sodium cations. Under the assumption that the quenched glasses represent the structural state of the melt near the glass transition temperature, the strong tendency of deuterium to concentrate as deuterosilanol (Si-OD) in a depolymerized Na-rich silicate network led to the conjecture that deuterium-enriched Na-Si-network fragments may be carried over to an exsolving silicate-saturated fluid, thus increasing the bulk D/H ratio of the coexisting fluid (Kueter et al., 2021).

The previous spectroscopic HDAC and NMR hydrogen isotope studies relied on heavily deuterium-enriched samples, which complicates their applicability to natural systems where deuterium constitutes less than 1 ‰ of the total hydrogen content. The present study constrains the intramolecular isotope effect in the hydrous NS4 system as a function of the bulk D/H ratio by using variously deuterium-enriched systems. Based on the very systematic behavior observed, we develop a model that constrains the intramolecular isotope effect with respect to deuterium concentration, which allows us to examine its relevance for variously hydrated sodium silicate melts at natural deuterium abundance.

2. Experimental and analytical techniques

2.1. Sample preparation and experimental protocol

Sodium tetrasilicate glass ("NS4", Na₂Si₄O₉) was synthesized from a 4:1 molar mix of spectroscopically pure SiO₂ and Na₂CO₃, previously dried for >24 h at 110 and 300 °C, respectively. Mixed powders were melted at 1400 °C for 30 min, crushed, and re-melted to ensure homogeneity of the glass product. Details on the preparation protocol are reported in Kueter et al. (2021). The dry-crushed and sieved (<200 μm) NS4 glass powder was used for subsequent experiments. To minimize water (i.e., H) contamination from hygroscopically attracted H₂O from air moisture, starting material and experimental products were stored at -80 °C in Ar-filled, paraffin-sealed glass vials. During analysis, the sample was further sealed inside the ZrO₂ rotor with Teflon spacers and cap. The pressurized air driving the NMR (nuclear magnetic resonance) rotor probe underwent three dehumidification steps before being introduced into the NMR system.

Platinum capsules (10×4 mm, length \times outer diameter) used for the solid-media, high-pressure experiments were loaded with water (H2O, D₂O or mix) with a microsyringe. The D₂O-H₂O water mixed solutions were previously created by mixing weight proportions of the pure reagents (D₂O, 99.9%, Cambridge Isotope Laboratories; H₂O milli-Q), then stored in Ar- and paraffin sealed vials at -80 °C before usage. Syringe needles were baked for 10 min at 300 °C to remove moisture prior to usage. The syringe was then flushed three times with the desired D2O-H₂O water mix before loading the capsule. All loading steps were monitored by weight, where water was loaded first, and based on its mass, dry NS4 powder was added to match a hydrous NS4 system with 8 wt% water. Capsules were crimped tight and bottoms cooled with a moist tissue envelope to prevent water evaporation from the capsule during welding with a PUK pulsed arc welder. Closed capsules were then immersed in acetone for a minimum of 24 h for leak testing. Postexperimental capsules were mechanically cleaned from adhered MgO pressure medium under a stereoscope using sharp needles. This way, MgO could be removed almost completely, with very little remains having no significant effect on the weight with respect to the precision of the balance. A strict weighing protocol between all preparation steps and after experiment traced potential contamination or loss;

Experiments with weight differences >1 mg were discarded.

Capsules were placed into 3/4-inch talc-Pyrex-MgO assemblies with a tapered graphite furnace (Kushiro, 1976) and loaded in a solid-media high-pressure apparatus (Boyd and England, 1960; Kushiro, 1976). The assembly parts were previously dried or fired overnight at 110 °C and 1000 °C, respectively. In all experiments, the temperatures were raised at a rate of 100 °C/min and ran at 1400 °C and 1.5 GPa for 2 h. Experiments were quenched under nearly isobaric conditions by turning off the power and simultaneously pumping oil to maintain the piston pressure. The reproducible rapid-quench rate of the high-pressure device is 70 °C s⁻¹ between dwell temperature and the glass transition at around 200 $^{\circ}\text{C}$ (Kueter et al., 2021). The temperature was controlled by a Watlow F4T thermocontroller using an S-type (Pt-Pt90-Rh10) thermocouple with no pressure correction for EMF. Uncertainties in temperature and pressure were \pm 10 °C and 0.1 GPa, respectively (Mysen, 2007b). The capsules were cleaned as outlined above, weighed, and either stored at $-80~^{\circ}\text{C}$ or directly opened for immediate NMR and Raman analysis.

2.2. NMR analyses

Glasses recovered from platinum capsules were powdered in a metal piston crusher and immediately analyzed with a Varian-Chemagnetics Infinity 300 solid-state NMR spectrometer at the Keck facility of the Earth and Planets Laboratory, employing a static magnetic field of 7.05 T. Sample powder were loaded in ZrO2 rotor probes (2.5 mm and 5.0 mm O.D. for $^1\mathrm{H}$ and $^2\mathrm{H}$, respectively). Protium ($^1\mathrm{H}$) NMR spectra acquisition was performed at a MAS probe spinning frequency ($\omega/2\pi$) of 22 kHz (drift is less than $\pm 20~\mathrm{Hz}$). RF coil $^1\mathrm{H}$ background suppression followed a DEPTH four pulse sequence. The acquisition was performed with a $^1\mathrm{H}$ 90° pulse length of 2.5 μs followed by a 10 s recycle delay to account for a $^1\mathrm{H}$ spin-lattice relaxation time of about 2 s. Spectral width was set to 200 kHz, and the spectra referenced with respect to tetramethylsilane defined as 0 ppm. A total of 8000 spectra were acquired per sample.

The ²H MAS NMR spectral acquisition was performed at a MAS frequency of 8 \pm 0.001 kHz. At this speed, ${}^{1}H^{-2}H$ homonuclear decoupling, e.g., in HDO molecules, is very weak and coupling between neighboring OH and OD groups even weaker. No difference in spectra was detected with or without using high power ¹H decoupling during signal acquisition, and the D NMR spectra were recorded, therefore, without high power ¹H decoupling. The D excitation pulse width was set to 1.5 μ s ($\omega_1/2\pi = 62.5$ kHz resulting in a 30° nutation angle), employing a recycle delay of 5 s resulted in no loss of signal to T₁ saturation effects. As the result of deuteron being a spin = 1 nucleus, typical ²H MAS NMR spectra are characterized by multiple sharp spinning sidebands spread over a wide frequency range, which result from rotational echoes arising from refocusing of the deuteron's quadrupole interaction once every rotor period, e.g., every 125 µs with 8 kHz MAS (Cody et al., 2020). From this complex spectral behavior, a purely isotropic ²H MAS NMR spectrum can be obtained by setting the MAS frequency to 8 \pm 0.001 kHz and the spectral width to 8 kHz while keeping the spectral filter width at 400 kHz. As a result, all spinning sidebands (that would reside outside of the spectral window) alias on top of each other, resulting in a purely isotopic spectrum that is comparable to those obtained from ¹H MAS NMR spectroscopy (Ashbrook and Wimperis, 2005; Eckman, 1982; Wang et al., 2015). To account for the intrinsic low signal strength for deuterium, 16,000 ²H MAS NMR spectra were acquired per sample. Spectral data are reported in the supplementary materials.

2.3. Raman analyses

Raman spectroscopic analysis was performed on glass shards recovered from the experiments. Glass shards were stored in sealed containers at $-80\,^{\circ}\text{C}$ prior to measurement as NS4 glasses are highly

hygroscopic and prone to structural re-equilibration if stored under ambient conditions (Kueter et al., 2021). Spectroscopic measurements were performed with a Jasco IRS-3100 confocal micro-Raman spectrometer using a 490 nm laser operating at about 31 mW at the sample. Spectra were recorded unpolarized with 600 grooves/mm (1300–4200 cm $^{-1}$ O-X stretch region) and 1200 grooves/mm (800–1300 cm $^{-1}$ structural region), 0.1 \times 6 mm slit, 60 s acquisition time and two iterations. Exact wavenumbers were calibrated against the 1332 cm $^{-1}$ signal of diamond.

Background corrections of Raman spectra were performed with the Wavemetrics IgorPro 8 mathematical software using the baseline package. A linear background correction was applied for spectra in the structural region for glasses by anchoring the baseline to the spectra at $830~\text{cm}^{-1}$ and $1300~\text{cm}^{-1}$. To correct the nominal D_2O content in the glasses detailed below, background corrections of the O-H and O-D signals at 3580 cm⁻¹ and 2650 cm⁻¹ were treated separately as a background treatment for the full, complexly-shaped water-region (1500-3800 cm⁻¹, Fig. 1) yields non-satisfactory results due to the complex shape of the spectrum. Background correction for the 2650 cm⁻¹ O—D resonance was performed with a linear function anchored at 2480 cm⁻¹ and 2750 cm⁻¹ because the low-frequency tail of the broad $3000~{\rm cm}^{-1}~{\rm O}$ —H stretch is superimposed on the low-frequency tail of the 3580 ${\rm cm}^{-1}$ maximum. A sigmoidal baseline correction was applied for the 3580 cm⁻¹ O—H stretch, applying integrations from 3000 to 3300 cm^{-1} for the low-frequency, and $3760 \text{ to } 3840 \text{ cm}^{-1}$ for the highfrequency spectral region bracketing the signal.

3. Results

3.1. Raman spectroscopy and correction for protium contamination

All experiments produced homogeneous silicate glasses devoid of quench bubbles, quench crystallization, or stable crystals. Raman spectra of hydrous NS4 glasses in the O—H and O—D primary vibrational stretch region (2000–4000 cm⁻¹) yield three bands with maxima at 3580 (2650) cm⁻¹, 3000 (2350) cm⁻¹, and 2350 (unknown) cm⁻¹ (O—D wavenumbers in brackets; Fig. 1), consistent with earlier studies

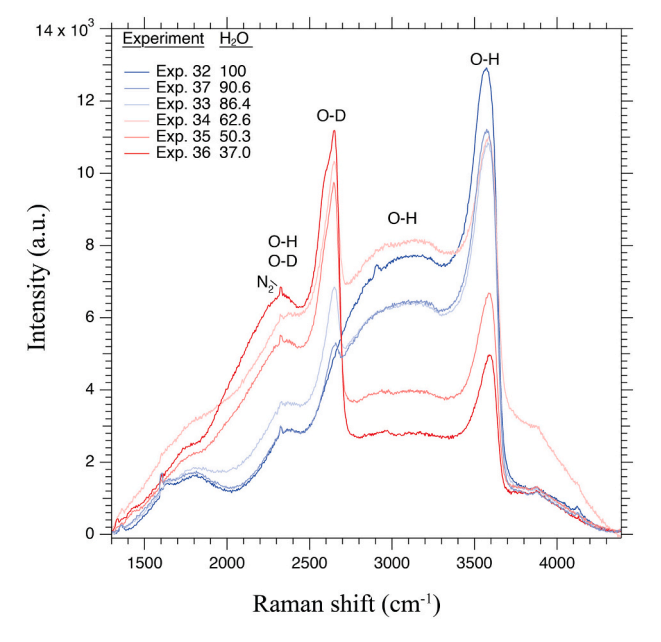


Fig. 1. Unpolarized Raman spectra of the O—H (O—D) stretching region. D to H exchange between experimental charge and assembly is apparent for the 100% $\rm D_2O$ experiment 36, yielding a strong I_{3580} O—H stretch band. $^1{\rm H}$ contamination is systematic and can be corrected (see text and supplementary information).

(Mcmillan et al., 1993; Zotov and Keppler, 1998). The intensity of the highest frequency stretching O-H and O-D bands at 3580 cm⁻¹ and 2650 cm^{-1} (I_{3580} and I_{2650}) correlate with the nominal concentrations of D₂O and H₂O. We observed a protium contamination issue in our deuterated experiments that is best illustrated with the nominal 100% D_2O experiment 36 (Fig. 1). A high I_{3580} for this indicates an influx of protium into the capsule at some point in the experiment. This contamination issue was also observed in an unrelated SiO₂-D₂O glass synthesis performed at similar experimental run conditions (Fig. S2). The simplest explanation would be that D2O and NS4 glass are hygroscopic or that H2O entered the capsule prior to welding (all options discussed in detail in the supplementary information). However, Raman spectroscopy on the D2O reagent yielded only a small contamination from H₂O that is too little to account for the O—H signal observed Exp. 36. Conservative estimates of contamination by water adsorbed on the NS4 glass powder amounts to <1.5 wt% additional H₂O and can thus not account for the excess in protium. Contamination of water during the welding process would have been detected by a mass gain, which was not observed. We conclude that diffusive exchange of hydrogen between the experimental charge and capsule exterior is the most likely cause of protium contamination. Platinum is permeable to hydrogen (Eugster, 1957; Richet et al., 1986) and contamination of the experimental charge by hydrogen from the capsule assembly is possible: During heating of the experiment, the talc of the pressure medium partly decomposes and inevitably releases water which reacts with the graphite heater to form a COH-fluid dominated by water (65 mol%) and significant amounts of H₂ (c. 5 mol%) (details in the supplementary materials). We suspect that H₂ diffuses into the experimental charge and participates in isotope exchange reactions with the experimental water, e.g., in the form of H₂ + $D_2O \Rightarrow HD + HDO$. Vice versa, HD and D_2 can permeate out of the capsule, and the bulk water or hydrogen content of the experimental charge remains preserved. To account for the protium contamination, a correction of the nominal D2O:H2O ratio was performed for all experiments. We tested two correction procedures: Method (i) correlates the I_{3580} to a linear correction function spanning between the I_{3580} of the nominal 100% H₂O experiment and a hypothetical null-intensity of I₃₅₈₀ at nominal 100% D₂O (Fig. S2a). Method (ii) projects the measured relative O—D intensity 2650 cm⁻¹ ($F_{I_{2650}} = I_{2650}/(I_{2650} + I_{3580})$) to a correction line constructed under the assumption of an ideal linear correlation the O-D and O-H intensities with the nominal H₂O and D₂O abundance in the system (Fig. S2b). Discrepancies between the two methods increase regarding the corrected D₂O content and range from 2.8 wt% difference in D₂O for the nominal 10% D₂O experiment 37 to 9 wt% for the nominal 100% D2O experiment 36. Method (i) yields thereby systematically higher D₂O abundances. We prefer method (i) as the I₃₅₈₀ has no interferences with O—D bands, while method (ii) suffers from insufficient separation of the OD and OH bands since the I_{2580} is situated on the tail of the I₃₀₀₀ O-H resonance. We do recognize the limitations of this method induced by the uncertainties on background correction and by sample compositional variability under constant instrumental parameters (Foustoukos and Mysen, 2013; Kagel, 1964). We also acknowledge the possibility of differing Raman scattering cross sections of protonated and deuterated species in the NS4 glass but assume that such differences are within the experimental uncertainty as reported from protonated and deuterated haplogranites (Zarei et al., 2018). The corrected H₂O and D₂O concentrations are reported in Table 1 and will be used in the following.

The Raman spectrum in the region where vibrations from silicate species occur (800–1300 cm $^{-1}$) is characterized by a prominent signal with an intensity maximum at $1070 \, \mathrm{cm}^{-1}$ (I_{1070} , Fig. 2a). This resonance is composed of underlying signals attributed to different Q-species composing the silicate melt structure (Le Losq et al., 2015a; Zotov and Keppler, 1998). Most prominent is the systematic increase of the I_{1070} with increasing bulk deuterium content. The difference spectrum in Fig. 2b also indicates the increase of underlying resonances at I_{1040} and the concomitant decrease of the I_{950} .

Table 1Hydrogen NMR results and intramolecular hydrogen isotope ratios.

Experiment	Nominal water*		Corrected Water**					¹ H NMR				² H NMR			Deuterium enrichment in alkali- associated network			
	H ₂ O	D ₂ O	H ₂ O	D ₂ O	wt% H ₂ O	wt% D ₂ O	$F_{(D_2O)}$	LF	LF ppm	HF	HF/ LF	LF	HF	HF/ LF	$lpha_{ ext{HF}/ ext{LF}}^{app}$		1σ	1000ln (α)
32	100	0	100.0	0.0	8.00	0.00	0.000	0.821	4.271	1.0	1.219							
37	90	10	90.6	9.4	7.25	0.75	0.094	0.867	4.372	1.0	1.154	0.563	1.0	1.776	1.54	\pm	0.05	431
33	75	25	86.4	13.6	6.91	1.09	0.136	1.001	4.860	1.0	0.999	0.593	1.0	1.688	1.69	\pm	0.05	524
34	50	50	62.6	37.4	5.01	2.99	0.374	1.094	4.960	1.0	0.914	0.492	1.0	2.033	2.22	\pm	0.05	799
35	25	75	50.3	49.7	4.02	3.98	0.497	1.198	5.648	1.0	0.835	0.482	1.0	2.073	2.48	\pm	0.05	910
36	0	100	37.0	63.0	2.96	5.04	0.630	1.360	5.550	1.0	0.735	0.467	1.0	2.143	2.92	\pm	0.05	1070

LF, HF: NMR Low-frequency (4-6 ppm) and high-frequency (16 ppm) signal intensity.

^{**} Actual water isotopologue concentration in glass after experiment. H₂O and D₂O wt% calculated on basis of 8 wt% total water in the system.

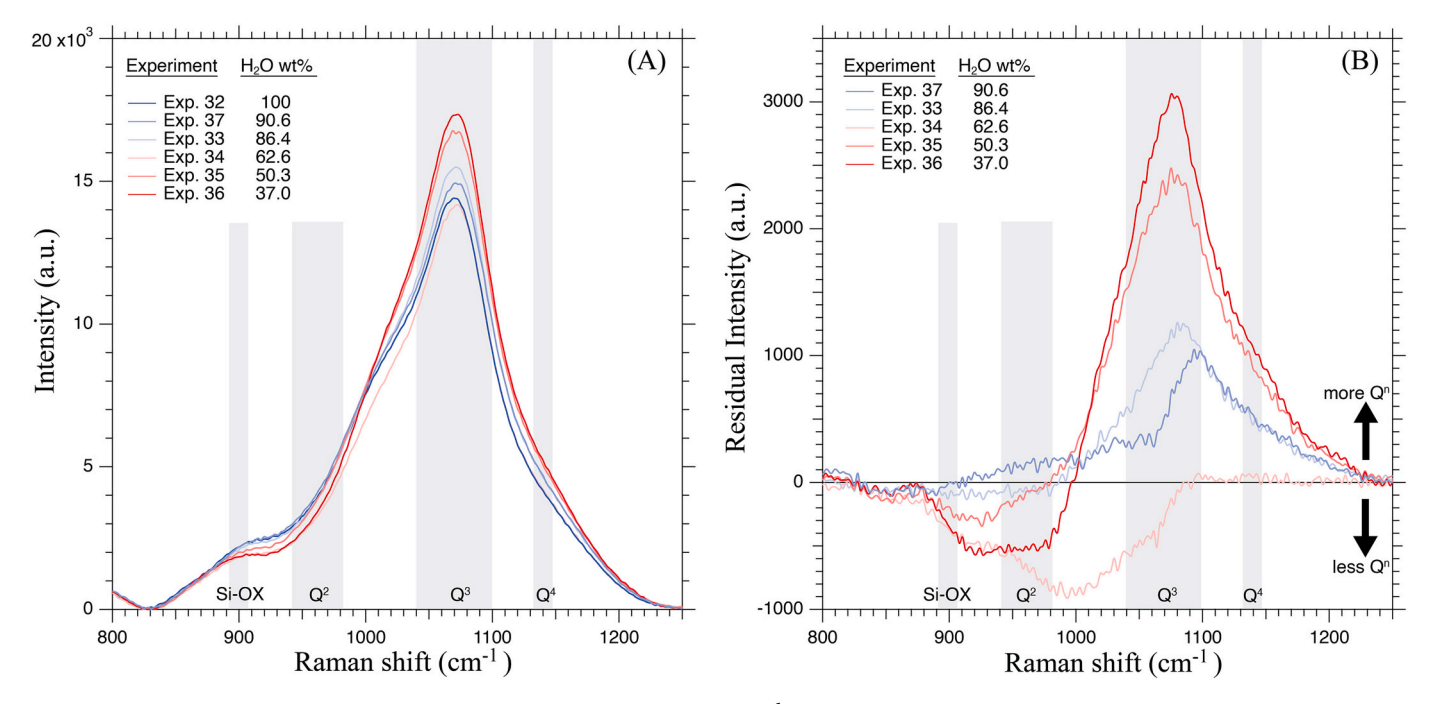


Fig. 2. A) Unpolarized Raman spectra of the structural region from 800 to 1250 cm^{-1} . Deuterium substitution causes a signal increase at wavenumbers corresponding to Q^3 and Q^4 Si—O stretching vibrations. B) A difference spectrum highlights the spectral variation upon deuteration. Deuterated sample spectra subtracted from $100\% \text{ H}_2\text{O}$ Experiment 32. Q^n -species assignment following Zotov & Keppler (1999) & LeLosq et al. (2015). Arrows indicate the increase or depletion of Q^n species relative to Exp. 32. A systematic increase of Q^3 and Q^4 species and a systematic decrease of Q^2 species are observed. Exp. 34 takes an outlier position in both figures due to larger fluorescence background resulting in lower intensities after background correction.

3.2. ¹H and ²H MAS NMR spectroscopy

From the perspective of hydrogen, both protium and deuterium occupy two structurally different environments in the NS4 tetrahedral network. This difference is reflected by the characteristic ¹H and ²H NMR double-peak spectra for hydrous alkali-silicate glasses, which comprise of a low-frequency (LF) resonance with an intensity maximum near 5 ppm and a high-frequency (HF) resonance with an intensity maximum at 16 ppm (Fig. 3)(Cody et al., 2005; Le Losq et al., 2015a; Robert et al., 2001; Schaller and Sebald, 1995; Wang et al., 2015; Xue and Kanzaki, 2004). Both signals are composed of at least two underlying resonances near 4 and 6 ppm and near 13 and 16 ppm (see Fig. 1 in Kueter et al., 2021 for details). The 13–16 ppm HF resonance is a typical feature found in alkali silicate glasses and is ascribed to predominantly structurally-bound hydrogen (Si-OX) and, to a lesser extent, to molecular water located near an alkali ion (Cody et al., 2005; Le Losq et al., 2015a; Robert et al., 2001; Schaller and Sebald, 1995; Xue and Kanzaki,

2001; Xue and Kanzaki, 2004). The 4-6 ppm LF resonance is a common feature in all hydrous SiO2 glasses, and its presence in alkali silicate glasses suggests hydrogen environments that are not directly influenced by alkali ions (Cody et al., 2005; Kohn et al., 1989; Wang et al., 2015). This signal is rather a feature of the hydrated (or deuterated) silicate network itself and the underlying 4 and 6 ppm contributions are the result of structurally bound (Si-OX) and molecular water (H₂O_m), respectively (Cody et al., 2020; Cody et al., 2005; Farnan et al., 1987; Kohn et al., 1989; Le Losq et al., 2015a; Schaller and Sebald, 1995; Xue and Kanzaki, 2001; Xue and Kanzaki, 2004). We term these two hydrogen environments the "alkali-associated silicate network" and the "alkali-free silicate network". Fig. 3 shows ¹H and ²H NMR spectra normalized with respect to the 16 ppm HF resonance. Deuteration systematically decreases the ¹H HF/LF intensity ratio and shifts the LF intensity maximum from 4 to 5.5 ppm. The latter indicates increased strength of the underlying 6 ppm resonance and thus higher H₂O_m content in the non-alkali-associated silicate network. The deuterium

LF ppm refers to chemical shift of the LF intensity maximum relative to the tetramethylsilane reference defined at 0 ppm.

¹σ uncertainty based on ²H NMR signal to noise ratio.

^{*} Initial water isotopologue concentration in starting material before experiment.

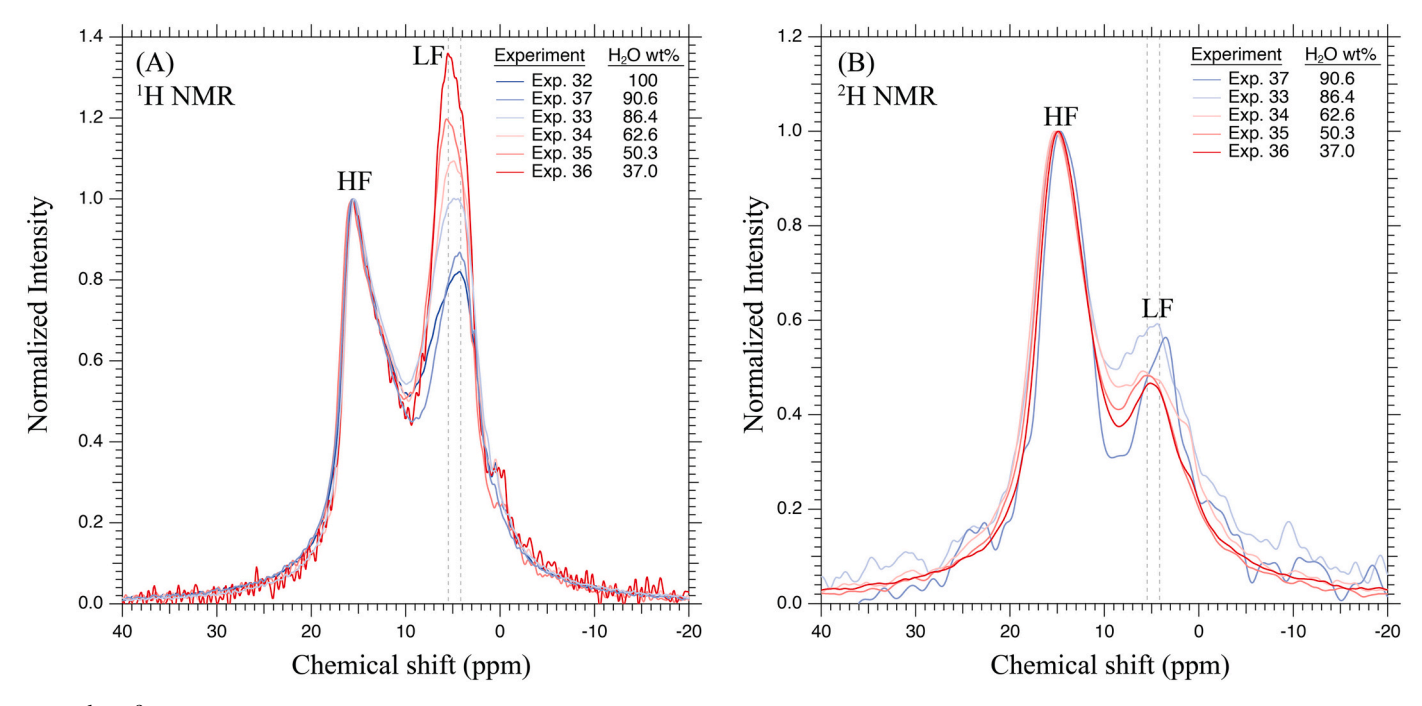


Fig. 3. 1 H & 2 H MAS NMR spectrum of hydrous sodium silicate classes. As the raw spectra yield varying signal strength, complicating interpretation, spectral data were normalized to 1 with respect to the 16 ppm HF intensity maximum. (A) Upon deuteration, the 1 H LF to HF intensity ratio (HF/LF)_H increases. The LF intensity maximum shifts from 4 to 5.5 ppm (dashed lines), indicating a larger signal contribution of the underlying 6 ppm resonance (1 POm, see text). (B) Deuteration of the system increases the HF to LF intensity ratio (HF/LF)_D. Note that the variation of the 2 H spectra is less pronounced compared to the 1 H spectra. Increasing signal noise is due to lower signal strength due to dilution of the respective isotope system.

spectrum in Fig. 3b shows a lesser but still systematic decrease in the 2H HF/LF ratio with increasing bulk D_2O/H_2O ratio. Given the larger signal-to-noise ratio and broader peak shape of the 2H spectra, no clear chemical shift of the 2H LF signal maximum is apparent. Fig. 5a displays a positive linear correlation between bulk isotope concentration and the $(HF/LF)_x$ ratio, where x stands for protium or deuterium.

4. Discussion

4.1. Isotope effect on the molecular glass structure

The state of polymerization of a silicate glass is described by the abundance of Q^n species, where n denotes the number of "bridging oxygens" connecting to another SiO₄ tetrahedron. A fully polymerized silicate network is composed of Q⁴ units, Q⁰ denotes isolated SiO₄ tetrahedra. Similarly, 4-n gives the number of non-bridging oxygens (NBO) to which hydrogen or alkalis can be bonded. Numerous studies correlated theoretical Raman normal mode calculations of silica anions as well as ²⁹Si NMR spectra with the high-frequency Raman resonances (800–1300 cm⁻¹) obtained from alkali-silicate glasses to reconstruct the individual Qⁿ speciation (Furukawa et al., 1981; Maekawa et al., 1991; Zotov and Keppler, 1998). Fig. 2a shows baseline-corrected Raman spectra in the structural region of hydrous NS4 glasses between 800 and $1300 \text{ cm}^{-1} \text{ with } Q^2 = 950 \text{ cm}^{-1}, Q^3 = 1040 - 1100 \text{ cm}^{-1} \text{ and } Q^4 = 1140$ cm⁻¹. The signal maximum is at 1070 cm⁻¹ (I_{1070}), consistent with previous studies on anhydrous NS4 glass (Furukawa et al., 1981) and NS4 glass with 8 wt% water (Zotov and Keppler, 1998). The pronounced shoulder near 900 ${\rm cm}^{-1}$ is assigned to Si-OX stretching or bending vibration and typically occurs in hydrated glasses, indicating a Si-O-Si + $X_2O \rightarrow 2$ Si-OX solution mechanism of water into the tetrahedral network of a silicate melt (Mcmillan et al., 1993; Zotov and Keppler, 1998). Based on reduced mass frequency calculations, a low-frequency shift of the I_{900} due to deuteration would be at maximum 20 cm⁻¹ and is not clearly resolved in our spectra.

While already apparent from Fig. 2a, differences in \boldsymbol{Q}^n speciation are

best displayed in the difference spectra in Fig. 2b, where the Raman spectra of deuterated experiments are subtracted from the 100% H2O spectrum of Exp. 32. Deuterium substitution generally causes systematic variation in the intensity of the main Raman signal. The increase of I_{1070} indicates a higher abundance of Q³ species in the silicate network, consistent with earlier experiments on isotopic endmembers (Le Losq et al., 2016; Zotov and Keppler, 1998). A concomitant decrease of the I_{950} intensity suggests lower concentrations of Q^2 species in the silicate melt structure. The evolution of the Q⁴ species is more ambiguous from the difference spectrum, and an apparent increase may in fact be the result of the rising Q³ signal. The increase of Q³ species is also apparent from the ²H NMR spectra. The relative intensity of the 16 ppm resonance, related to Q³ species based on ¹H—²⁹Si cross-correlation NMR (Robert et al., 2001), rises with increasing bulk D₂O/H₂O ratios. This suggests a higher concentration of deuterated Q³ species nearby the sodium ion (Fig. S3).

Generally, the disproportionation equilibrium

$$2O^{n} = O^{n-1} + O^{n+1} (1)$$

is well documented in alkali silicate melts and shifts to the left side if either alkali concentration increases (Maekawa et al., 1991) or alkali ionic radius decreases (Mysen, 1997; Mysen and Richet, 2018). In light of the intensity changes caused by D_2O and H_2O , we suggest that increasing deuteration drives the reaction $2Q^3=Q^2+Q^4$ to the left-hand side.

While variations in the bulk Q^n speciation can be resolved by Raman spectroscopy, it cannot provide information on the locality of the isotope substituted species. Here, hydrogen NMR provides additional insights. The 16 ppm resonance has been previously related to Q^3 species based on $^1H^{-29}$ Si cross-correlation NMR (Robert et al., 2001), and by comparison with alkali-free hydrous silicate glasses, we can deduce that these Q^3 species must be in relation with alkali ions dissolved in the silicate network. Increasing deuteration leads to a relative increase in HF intensity (Fig. S3), suggesting a higher concentration of deuterated Q^3 species nearby the sodium ion. 1H NMR spectra show that increasing

deuteration also leads to a relative increase of protium concentration in the non-alkali associated network, as indicated by a relative increase of the LF intensity (Fig. 3a). A concomitant chemical shift of the LF intensity maximum from 4 to 6 ppm indicates that protium is increasingly stored as H₂O_m rather than Si-OH (Xue and Kanzaki, 2004). It appears from this observation that deuteration forces the H to D substitution from Si-OH to Si-OD and potentially the formation of new Si-OD, consistent with earlier zero-point energy (ZPE) considerations (Kueter et al., 2021). The preference of deuterium to bond with alkali-associated Q³ species has also been observed in Li and K tetrasilicate glasses (LS4, KS4), where it was shown that the ²H NMR HF signal in deuterated LS4 and KS4 glasses is consistently stronger relative to the respective ¹H NMR HF signal (Le Losq et al., 2016). This is the case even if the total abundance of alkali-associated Q3 species is very low such as in the hydrous LS4 glasses (Le Losq et al., 2015b). This preference for deuterium to bond with Si-OX near alkali ions suggests that non-bridging oxygens in Qⁿ species are energetically nonequivalent within the silicate melt structure and network-internal differences in the Si-OX (NBO-X) bonding energies eventually lead to intramolecular isotope effects. The presence of energetically non-equivalent oxygen has also been deduced from the preference of network modifying cations to bond with specific NBO, causing local ordering of the network (Huang and Cormack, 1991; Mysen and Richet, 2018), and has been inferred from element partitioning studies between crystals and melts (Mysen, 2007a).

4.2. Intramolecular hydrogen isotope exchange

Intramolecular hydrogen isotope exchange can take place between various hydrogen-bearing environments in the silicate melt/glass structure, for example, among the hydrated Qⁿ species and between Qⁿ species and molecular water. It is not possible to determine the many possible exchange mechanisms among the multitude of hydrogen environments within the silicate melt, but NMR spectroscopy allows quantification of the general hydrogen isotope exchange between the *alkaliassociated silicate network* and the *alkali-free silicate network*. For this, the intensity ratios of the ¹H and ²H NMR high-frequency (HF) and low-frequency (LF) resonances are used to calculate an apparent fractionation factor (Wang et al., 2015):

$$\alpha_{HF/LF}^{app} = \frac{(D/H)_{HF}}{(D/H)_{LF}} = \begin{pmatrix} I_{HF}^D \\ I_{LF}^D \end{pmatrix} \bullet \begin{pmatrix} I_{LF}^H \\ I_{HF}^H \end{pmatrix}$$
 (2)

As visible from Fig. 4, $\alpha_{HF/LF}^{qpp}$ correlates positively with increasing bulk D/H ratio. Relative deuterium concentrations in the alkali-

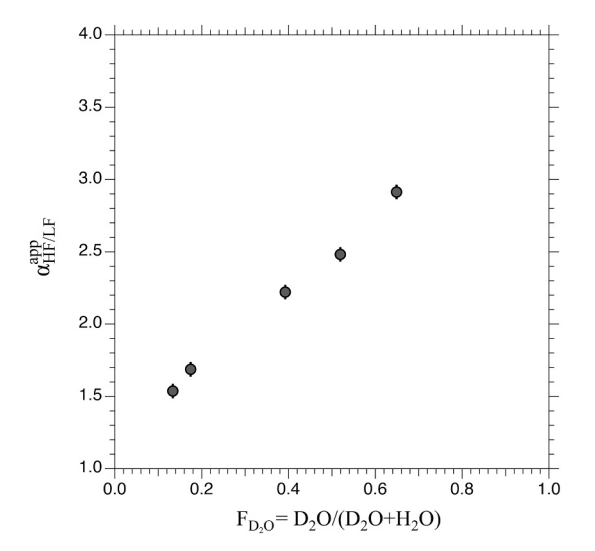


Fig. 4. Positive correlation of $\alpha_{HF/LF}^{app}$ with the bulk D₂O fraction (F_{D2O}) in the NS4 melt. Symbol errors are 1σ .

associated network increase from $\alpha_{HF/LF}^{app}$ 1.5 at 9.4% D_2O to 2.9 at 63% D_2O in the glass (Table 1). The observed dependency of $\alpha_{HF/LF}^{app}$ with isotope concentration is unique to the quenched melt-only system and is, to our knowledge, not observed in other two-phase isotope fractionation studies. In-situ HDAC experiments on D/H exchange between alumosilicate melts and coexisting aqueous fluids of differing D/H ratios (0.05 to 2.68) also showed no systematic dependency of $\alpha_{fluid\text{-melt}}$ and deuterium concentration (Dalou et al., 2015). More generally, and similar to chemical equilibrium constants, isotope fractionation factors should be invariant to variations in isotope concentrations.

Eckert et al. (1988) and later Xue and Kanzaki (2001, 2004) showed that variation in O—H bond lengths leads to ¹H chemical shifts, where greater O—H bond distances correlate with higher ¹H chemical shifts in frequency. Eckert et al. (1988) found a strong linear correlation between O-H···O bond distances with ¹H chemical shift obtained by standards that could indicate 0.25 and 0.3 nm diameter cavities for H or D in the HF and LF regions, respectively. This relationship led others to consider that intramolecular D/H fractionation was linked to the different O-H and O-D bond lengths (Si-O-X···O-Si) in the alkali-associated and alkali-free silicate network (Le Losq et al., 2016; Wang et al., 2015). Taken as a measure for the available molecular volume to host the hydrogen isotope, Wang et al. (2015) proposed that there might be a molar volume isotope effect (MVIE) in which deuterium preferentially partitions to the lower-volume site associated with the alkali ion. Relatedly, Le Losq et al. (2016) referred to "different 'effective' ionic radii of ¹H and ²H", though remaining unclear about the expected direction of isotopic fractionation. The effective ionic radius for the H anion is 139.9 nm (Lang and Smith, 2010), but it is to our knowledge unconstrained for the D⁻ anion, so this hypothesis remains to be tested. In our preceding study, we argued for an underlying classical isotope effect that roots in the varying vibrational ground states (i.e., ZPE) of the individual hydrous entities (Kueter et al., 2021). Here, O-X configurations (mostly silanols) in the alkali-associated silicate network are markedly stronger than O-X configurations in the non-alkali associated network (i.e., silanols, H₂O_m, M-OX), in line with the presence of energetically non-equivalent Q-species mentioned above.

In Kueter et al. (2021), we demonstrated that quench-decompression from different synthesis pressures introduces a systematic kinetic isotope effect (KIE) in hydrous NS4 glasses that systematically affect $a_{HF/LF}^{app}$. It was observed that the $a_{HF/LF}^{app}$ value grew larger the lower the synthesis pressure was. This was explained by an increased efficiency of the silanol condensation reaction (2 Si-OX \rightarrow Si-O-Si + X₂O) at lower total pressures and for the protonated compared to deuterated silanols. The thus formed excess H₂O species contributes to the LF region in the 1 H NMR spectrum, increasing the $lpha_{HF/LF}^{app}$ value. In the same study, a lowpressure experiment then demonstrated that near-isobaric quenching lowered $\alpha_{HF/LF}^{app}$ to values similar to the high-pressure syntheses. This indicates that silanols are stabilized with pressure, and silanolcondensation is prevented when the system is quenched while maintaining synthesis pressure, diminishing a KIE contribution. The experiments of the present study were quenched near-isobaric, thus a significant contribution of a KIE to $\alpha_{\rm HF/LF}^{\rm app}$ is not expected.

Overall, it is possible that all mentioned isotope effects, and such yet undescribed, contribute to the observed apparent intramolecular hydrogen isotope effect. The apparent intramolecular hydrogen isotope *fractionation* has, thus, more in common with an element *partitioning* factor as being an empirical measure for the numerous physical and chemical variables that drive the D to H separation in the system. If we (i) view the alkali-associated and non-alkali-associated silicate network as two phases with different capacities to incorporate hydrogen and (ii) look at protium and deuterium individually, we find a positive correlation between isotope concentration and "partitioning" into the alkali-

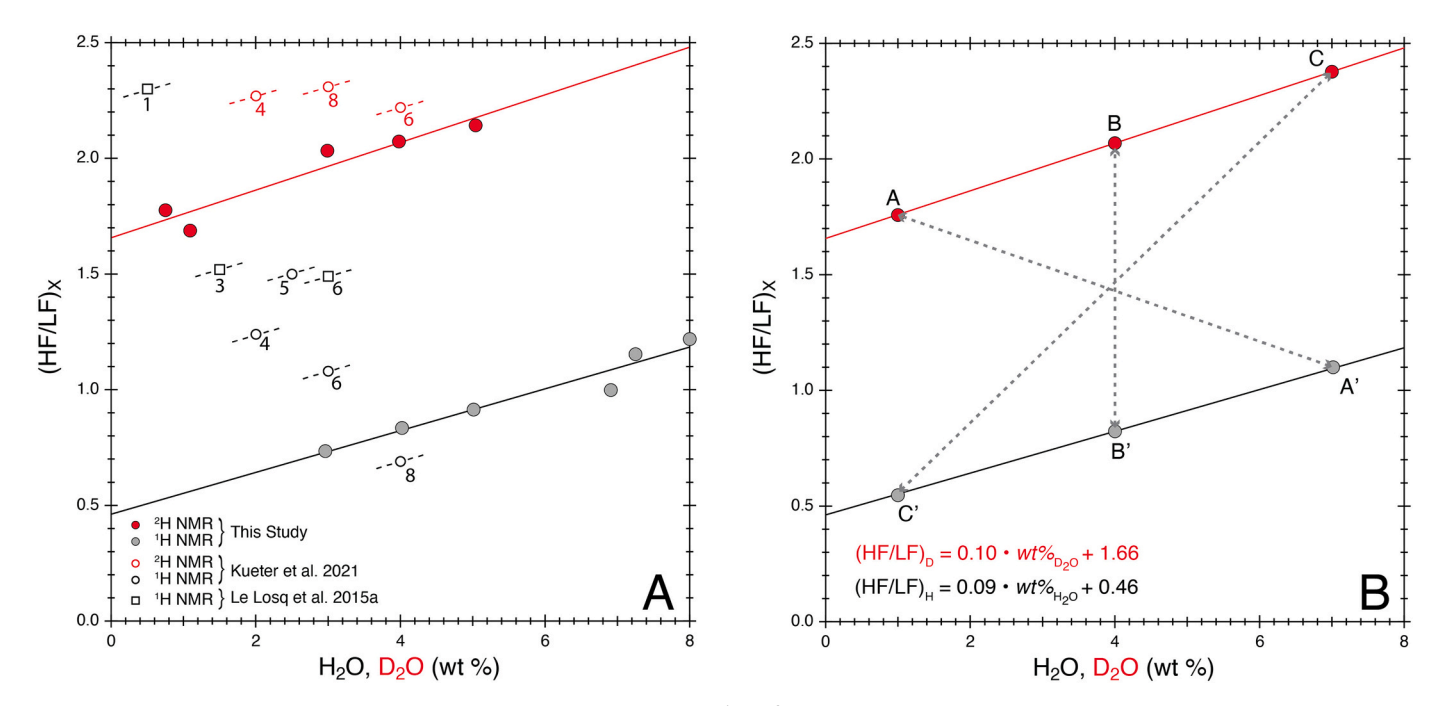


Fig. 5. A) Relationship between relative HF intensity (HF/LF intensity ratio, $X = {}^{1}H$ or ${}^{2}H$ NMR) and isotope concentration, expressed as weight percentage $H_{2}O$ or $D_{2}O$. Experiments define nearly parallel running linear regressions (see equations in panel B). Open symbols are experiments with 1:1 $D_{2}O/H_{2}O$ but different bulk water contents as annotated by numbers (wt% total water). Lower bulk water contents drive particularly protium to higher partition values. Dashed lines behind symbols assume linear trendlines parallel to the solid-line regressions used for the model in Fig. 5 (see text). Note that these experiments were not corrected for H-contamination. B) Model explaining the isotope concentration dependency of $\alpha_{HF/LF}^{app}$, which becomes larger when the bulk $D_{2}O/H_{2}O$ ratio increases. Case A, 1 wt% $D_{2}O$ and 7 wt% $D_{2}O$ and 7 wt% $D_{2}O$ gives $D_{2}O$ gives $D_{2}O$ gives $D_{2}O$ gives $D_{2}O$ gives $D_{2}O$ gives $D_{2}O$ and 1 wt% $D_{2}O$ and 1 wt%

associated network (Fig. 5a). Based on the regressions for both hydrogen isotopes, we can define linear "partition functions" of type y = mx + b, which ratio can describe $\alpha_{HF/LF}^{app}$ for every D_2O/H_2O ratio in an NS4 system with 8 wt% bulk water ($wt\%_{bulk}$):

$$\alpha_{HF/LF}^{app} = \frac{m_D(wt\%_{bulk} - wt\%_{H_2O}) + b_D}{m_H(wt\%_{H_2O}) + b_H}$$
(3)

This equation shows that for varying bulk D₂O/H₂O ratios (x term, based on wt%), $\alpha_{HF/LF}^{app}$ is defined by the slope (m term) of the deuterium and protium partition functions as well as the intercept (b term). As illustrated by the dashed tie lines in Fig. 5b, low concentrations in D and high concentrations in H result in a low $\alpha_{HF/LF}^{app}$, while increasing the bulk D₂O/H₂O results in an increased $\alpha_{HF/LF}^{app}$ value. The limits that give us the maximum site partitioning of each isotope near 100% abundance are $\lim_{D_2O-8wt\%}\alpha_{HF/LF}^{app}\approx 5.3$ and $\lim_{H_2O-8wt\%}\alpha_{HF/LF}^{app}\approx 1.4$ (Fig. 6). The latter value is particularly interesting as it essentially reflects the deuterium partitioning into the alkali-associated silicate network near natural deuterium abundance, i.e., a bulk D/H ratio of 1.56×10^{-4} . In other words, for this system at natural D/H composition, deuterium is enriched by a factor of 1.4 in the alkali-associated silicate network.

To explore how lower bulk water concentrations affect the $\alpha_{HF/LF}^{app}$ value, earlier NS4 experiments with 1 to 8 wt% bulk water are shown in Fig. 5a (Kueter et al., 2021; Le Losq et al., 2015a). Note that these experiments are not corrected for protium contamination and were quenched non-isobaric, which has an effect on the HF/LF and $\alpha_{HF/LF}^{app}$ values (e.g., Kueter et al., 2021, cf., pressure series). We can observe that the (HF/LF)_H increases for protonated glasses from high to low bulk

water content. Systematic variations in (HF/LF)_D is not apparent. A possible interpretation for the correlation of (HF/LF)_H and bulk water content may be that the NS4 system has, at given P-T and in simplified terms, a fixed number of structural hydrogen positions (i.e., Si-OX) in the alkali-associated network. As known from previous hydrogen NMR studies, deuterons preferably bond with the alkali-associated silicate network, as reflected by consistently high $^2\mathrm{H}$ NMR HF/LF-ratios (Kueter et al., 2021; Le Losq et al., 2016; Wang et al., 2015). These positions are more readily available for both hydrogen isotopes at lower total water content, thus diminishing the competition of deuterons and protons for such sites. Consequently, at constant bulk D₂O/H₂O ratio, $\alpha_{HF/LF}^{app}$ should decrease when the bulk water content decreases, which is in fact observed for the 1:1 D₂O:H₂O NS4 system (Fig. 7 in Kueter et al., 2021).

The dashed lines in Fig. 6 show how $\alpha_{HF/LF}^{app}$ varies as a function of bulk D₂O/H₂O ratio and variable bulk water content in the melt. The calculation of these lines is based on a similar model as displayed in Fig. 5 using the weight fraction of $D_2O(F_{D2O})$ instead of absolute values. and takes the data of Kueter et al. (2021) into account (Details in supplementary materials). Note that the apparent offset for the two bulk 8 wt% water experiments is likely because experiments in both studies were quenched differently (non-isobaric vs. nearly isobaric in this study) and the previous data were not corrected for protium contamination. The main conclusions from Fig. 6 are that (i) for any given bulk water content, $\alpha_{HF/LF}^{app}$ correlates positively with the bulk D₂O/H₂O ratio, and (ii) at natural deuterium abundance, deuterium partition into the alkaliassociated silicate network increases with an increasing bulk water content of the melt. This interpretation appears generally corroborated by the data of Wang et al. (2015), which also shows a positive correlation between $\alpha_{HF/LF}^{app}$ and bulk water content (Fig. 6, asterisk symbols). However, we note that the extrapolation to NS4 systems with bulk water contents other than 8 wt% requires further experimental backup.

¹ Not to confuse with the molecular partition function Q used to calculate theorectical fractionation factors, e.g., Richet et al., 1977.

Chemical Geology 610 (2022) 121076

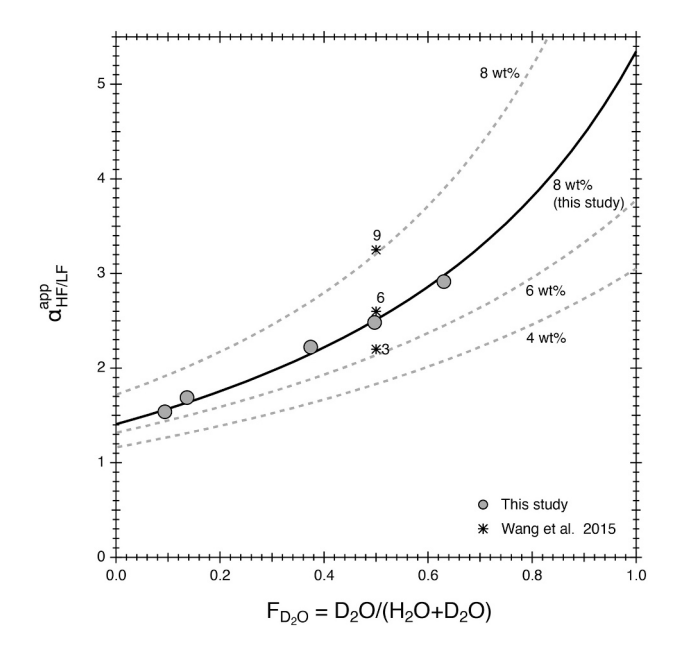


Fig. 6. Change of the intramolecular hydrogen isotope partitioning factors as a function of the D_2O fraction (F_{D2O}). The solid line is calculated from the model presented in Fig. 4 (see text) and based on the experiments of this study. Dashed partitioning curves are derived from previous experiments (Kueter et al., 2021), assuming a similar linear behavior of the HF/LF intensity ratios and isotope concentration (see text and supplementary information). Note that these experiments were not corrected for protium contamination, likely explaining the discrepancy of the two 8 wt% curves. $\alpha_{HF/LF}^{app}$ decreases with decreasing bulk water content. The 0-intercept of the y-axis approximates the deuterium partitioning into the alkali-associated network at natural deuterium abundance, i. e., D/H or (F_{D2O}) $\approx 1.56 \times 10^{-4}$. Asterisk-symbols are 1:1 D_2O/H_2O NS4 glasses synthesized by Wang et al. (2015), showing the same trend to lower $\alpha_{HF/LF}^{app}$ with decreasing bulk water content (number annotation in wt%). Note that these experiments were also not corrected for protium contamination; high-deuterium experiments are therefore not shown.

4.3. Intramolecular hydrogen isotope partitioning at natural deuterium abundance

To put this large intramolecular hydrogen partitioning into perspective, it is useful to compare $\alpha_{HF/LF}^{app}$ to D/H fractionations observed in natural and synthetic two-phase systems. Because $\alpha_{A/R}$ in two-phase systems are usually very close to unity, it is common to express fractionations as 10^3 ln $\alpha_{A/B}$ values, which for the sake of readability, are expressed in permil (%). This convention is less suitable for α much larger than unity but is applied here to allow for a better comparison of our experimental results with two-phase hydrogen isotope fractionation factors. A compilation of typical hydrogen isotope fractionations in comparison to intramolecular hydrogen fractionations in alkali silicate glasses is shown in Fig. 7. Typical hydrogen isotope fractionations in the vapor-melt system amount to <50 % deuterium enrichment in the gas phase (Dobson et al., 1989; Pineau et al., 1998; Richet et al., 1986). Equally small fractionations (<100 %) are observed for experimental water-mineral pairs (Saccocia et al., 2009; Suzuoki and Epstein, 1976) and H₂-mineral (or mineral-mineral) pairs (Vennemann and ONeil, 1996). Larger two-phase hydrogen isotope fractionations are known from the CH₄ - H₂ and H₂O - H₂ systems (Horibe and Craig, 1995; Richet et al., 1977). Fractionations of up to 700 % have been reported from insitu hydrothermal diamond anvil experiments in the Na-(Al)-Si-X2O system (Dalou et al., 2015; Mysen, 2013a; Mysen, 2013b). Previous NMR studies on quenched alkali silicate melts suggested intramolecular hydrogen effects of significantly larger magnitude than observed for two-phase systems, averaging at around 1000 % deuterium enrichment in the alkali-associated silicate network (Kueter et al., 2021; Le Losq

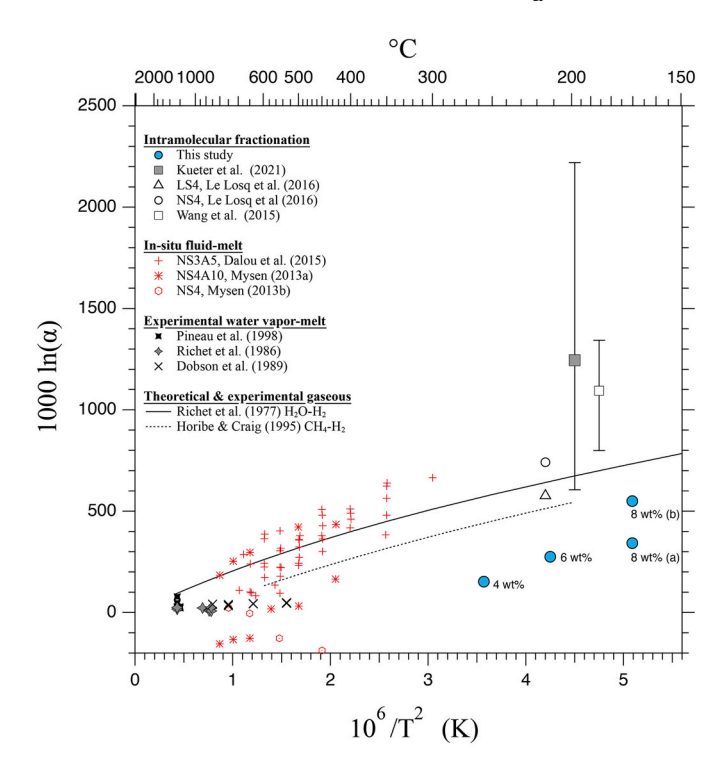


Fig. 7. Comparison of intramolecular deuterium enrichment in the alkaliassociated network relative to hydrogen isotope fractionations observed in two-phase systems. The intramolecular isotope partitioning is captured at the glass transition temperature (T_g), which for hydrous alkali silicate glasses with 3–8 wt% is around 200 °C (Behrens and Yamashita, 2008). Observed Intramolecular partitioning factors are likely to fall in this temperature range. Corresponding experiments by Le Losq et al. (2016), Wang et al. (2015), and Kueter et al. (2021) are plotted offset to another for better visibility and are not T_g estimates. Bars correspond to the range of $\alpha_{HF/LF}^{app}$ values observed in the respective studies. Blue symbols are $\alpha_{HF/LF}^{app}$ values for natural deuterium abundance calculated based on the isotope-concentration model described in the text and Fig. 5. Datapoint annotation refers to bulk water content (8 wt% (a) = this study, (b) = Kueter et al., 2021). T_g estimates for these data points are based on Behrens and Yamashita (2008). (For interpretation of the references to colour in this figure legend, the reader is referred to the web version of this article.)

et al., 2016; Wang et al., 2015). In light of the present study, such large intramolecular isotope effects cannot be compared to natural systems as we have demonstrated a strong correlation of $\alpha_{HF/LF}^{app}$ with the bulk D₂O/ H₂O ratio in the melt. Our present model for an NS4 system with 8 wt% bulk water suggests ~340 % deuterium enrichment in an alkaliassociated silicate network at natural deuterium abundance and at the temperature of the glass transition (c. 170 \pm 40 °C, extrapolated from Behrens and Yamashita, 2008). Our previous data for NS4 melts with 4, 6, and 8 wt% bulk water suggest intramolecular deuterium enrichment in the alkali-associated silicate network by 150 to 540 ‰ for glass transition temperatures between 250 \pm 40 to 170 \pm 40 $^{\circ}\text{C},$ respectively. As seen in Fig. 7, the magnitude of these values appears in much better agreement with hydrogen isotope fractionations observed in natural two-phase systems. They are also notably consistent with the bulk D/H fractionations between hydrous Na-(Al)-Si melt – silica-saturated fluid under pressure (Dalou et al., 2015; Mysen, 2013a; Mysen, 2013b).

In Kueter et al. (2021), we suggested that higher D/H ratios in alkalirich domains could carry over into a coexisting silicate-saturated fluid phase, e.g., when a hydrous melt separates into two liquids. The similarity between intramolecular D/H fractionation and hydrous melt – silicate saturated fluid fractionation supports this model. The apparent increase of the isotope effect with rising water content is thereby particularly interesting, as it indicates a higher efficiency of deuterium separation into the fluid phase in environments where hydrous melts are

common, e.g., in subduction settings. As a consequence, the separation of a hydrous fluid phase from a water-saturated melt under pressure may be the most effective step in the deep water cycle to separate hydrogen isotopes. It could thus be a major driver for the continuous D/H increase of the Earth's surface oceans.

5. Conclusion

Hydrogen isotopes in hydrous alkali silicate melt partition preferentially into the silicate network sites that are associated with alkali ions. This partitioning is stronger for deuterium than it is for protium, which gives rise to an intramolecular hydrogen isotope effect resolvable by NMR spectroscopy. The intramolecular hydrogen isotope exchange is strongly dependent on isotope concentration and total water concentrations in the NS4 system, and thus resembles a partitioning factor rather than a classical isotope fractionation factor. The intramolecular deuterium partitioning into the alkali-associated silicate network increases thereby towards higher bulk D₂O/H₂O ratios and increasing bulk water content. Modeling of the concentration-dependent isotope effect suggests 150 to 540 % deuterium enrichment in the alkali-associated silicate network at natural D/H abundance, depending on bulk water content. These deuterium enrichments are significantly lower than previously suggested but much more consistent with the general magnitude of hydrogen isotope fractionations in two-phase systems. They are also in agreement with earlier in-situ HDAC fractionation studies in the Na-(Al)-Si-water system, indicating a link between deuterium fractionation processes taking place inside the silicate melt structure and the macroscopic fractionation of hydrogen isotopes in twoliquid systems. Still, the role of the alkali identity, mixtures, alkali/SiO₂ ratio, and bulk water content on the intramolecular hydrogen isotope effect remains to be studied in greater detail. Also unknown remains the role of network-forming elements beyond Si. Building on such fundamental constraints, models on intramolecular hydrogen isotope partitioning can be developed for chemically more complex systems. Such models will provide insights into the hydrogen isotope exchange in the extreme environments inside Earth, thus helping us to constrain the pathways of the deep Earth water cycle.

Declaration of Competing Interest

The authors declare that they have no known competing financial interests or personal relationships that could have appeared to influence the work reported in this paper.

Data availability

Research data can be found in the supplementary information.

Acknowledgements

The authors like to thank Dr. Emma Bullock for microprobe support as well as Joseph Lai and Javier Rojas for technical support. We further thank Celia Dalou and an anonymous reviewer for their constructive comments and Sonja Aulbach for editorial handling. This project was funded by a Carnegie Postdoctoral Fellowship awarded to NK. We acknowledge the NSF EAR-1761388 grant awarded to DF.

Appendix A. Supplementary data

Supplementary data to this article can be found online at https://doi.org/10.1016/j.chemgeo.2022.121076.

References

- Ashbrook, S.E., Wimperis, S., 2005. Rotor-synchronized acquisition of quadrupolar satellite-transition NMR spectra: practical aspects and double-quantum filtration. J. Magn. Reson. 177 (1), 44–55.
- Behrens, H., Yamashita, S., 2008. Water speciation in hydrous sodium tetrasilicate and hexasilicate melts: Constraint from high temperature NIR spectroscopy. Chem. Geol. 256 (3–4). 306–315.
- Boyd, F.R., England, J.L., 1960. Apparatus for Phase-Equilibrium Measurements at pressures up to 50-Kilobars and Temperatures up to 1750 °C. J. Geophys. Res. 65 (2), 741–748
- Chacko, T., Cole, D.R., Horita, J., 2001. Equilibrium oxygen, hydrogen and carbon isotope fractionation factors applicable to geologic systems. Stable Isotope Geochemistry 43, 1–81.
- Cody, G.D., Mysen, B.O., Lee, S.K., 2005. Structure vs. composition: a solid-state ¹H and ²⁹Si NMR study of quenched glasses along the Na₂O-SiO₂-H₂O join. Geochim. Cosmochim. Acta 69 (9), 2373–2384.
- Cody, G.D., Ackerson, M., Beaumont, C., Foustoukos, D.I., Le Losq, C., Mysen, B.O., 2020.
 Revisiting Water Speciation in Hydrous Alumino-Silicate glasses: a Discrepancy between Solid-state ¹H NMR and NIR spectroscopy in the Determination of X-OH and H₂O. Geochim. Cosmochim. Acta 285. 150–174.
- Dalou, C., Le Losq, C., Mysen, B.O., 2015. In situ study of the fractionation of hydrogen isotopes between aluminosilicate melts and coexisting aqueous fluids at high pressure and high temperature - Implications for the δD in magmatic processes. Earth Planet. Sci. Lett. 426, 158–166.
- Dobson, P.F., Epstein, S., Stolper, E.M., 1989. Hydrogen Isotope Fractionation between Coexisting Vapor and Silicate-Glasses and Melts at Low-pressure. Geochim. Cosmochim. Acta 53 (10), 2723–2730.
- Eckert, H., Yesinowski, J.P., Silver, L.A., Stolper, E.M., 1988. Water in Silicate-Glasses Quantitation and Structural Studies by ¹H Solid Echo and MAS-NMR Methods. J. Phys. Chem. 92 (7), 2055–2064.
- Eckman, R.R., 1982. Hydrogen and Deuterium NMR of Solids by Magic Angle Spinning. University of California, Berkeley, Berkeley.
- Eugster, H.P., 1957. Heterogeneous Reactions Involving Oxidation and Reduction at High pressures and Temperatures. J. Chem. Phys. 26 (6), 1760–1761.
- Farnan, I., Kohn, S.C., Dupree, R., 1987. A Study of the Structural Role of Water in Hydrous Silica Glass using Cross-Polarization Magic Angle Spinning NMR. Geochim. Cosmochim. Acta 51 (10), 2869–2873.
- Foustoukos, D.I., Mysen, B.O., 2013. H/D methane isotopologues dissolved in magmatic fluids: Stable hydrogen isotope fractionations in the Earth's interior. Am. Mineral. 98 (5–6), 946–954.
- Furukawa, T., Fox, K.E., White, W.B., 1981. Raman spectroscopic investigation of the structure of silicate glasses. III. Raman intensities and structural units in sodium silicate glasses. J. Chem. Phys. 75 (7), 3226–3237.
- Horibe, Y., Craig, H., 1995. D/H fractionation in the system methane-hydrogen-water. Geochim. Cosmochim. Acta 59 (24), 5209–5217.
- Huang, C.D., Cormack, A.N., 1991. Structural differences and Phase-Separation in Alkali Silicate-Glasses. J. Chem. Phys. 95 (5), 3634–3642.
- Kagel, R.O., 1964. Vibrational Intensity Studies. (Parts I and II). University of Minnesota. Kohn, S.C., Dupree, R., Smith, M.E., 1989. Proton Environments and Hydrogen-Bonding in Hydrous Silicate-Glasses from Proton NMR. Nature 337 (6207), 539–541.
- Kueter, N., Cody, G.D., Foustoukos, D.I., Mysen, B.O., 2021. Hydrogen isotope fractionation inside silicate melts and glasses studied by ¹H and ²H MAS NMR spectroscopy - Molecular insights into deuterium exchange at the melt-fluid interface. Geochim. Cosmochim. Acta 309, 171–190.
- Kurokawa, H., Foriel, J., Laneuville, M., Houser, C., Usui, T., 2018. Subduction and atmospheric escape of Earth's seawater constrained by hydrogen isotopes. Earth Planet. Sci. Lett. 497, 149–160.
- Kushiro, I., 1976. A new furnace assembly with a small temperature gradient in solid-media, high-pressure apparatus. Carnegie Institution of Washington Year Book 75, 832–833.
- Lang, P.F., Smith, B.C., 2010. Ionic radii for Group 1 and Group 2 halide, hydride, fluoride, oxide, sulfide, selenide and telluride crystals. Dalton Trans. 39 (33), 7786–7791.
- Le Losq, C., Cody, G.D., Mysen, B.O., 2015a. Alkali influence on the water speciation and the environment of protons in silicate glasses revealed by ¹H MAS NMR spectroscopy. Am. Mineral. 100 (2–3), 466–473.
- Le Losq, C., Mysen, B.O., Cody, G.D., 2015b. Water and magmas: Insights about the water solution mechanisms in alkali silicate melts from infrared, Raman, and ²⁹Si solidstate NMR spectroscopies. Progress in Earth and Planetary Science 2.
- Le Losq, C., Mysen, B.O., Cody, G.D., 2016. Intramolecular fractionation of hydrogen isotopes in silicate quenched melts. Geochemical Perspectives Letters 2 (1), 87.
- Lecuyer, C., Fourel, F., Blamey, N., Brand, U., Fralick, P.W., 2020. 8²H of water from fluid inclusions in Proterozoic halite: evidence for a deuterium-depleted hydrosphere? Chem. Geol. 541.
- Maekawa, H., Maekawa, T., Kawamura, K., Yokokawa, T., 1991. The Structural groups of Alkali Silicate-Glasses Determined from ²⁹Si MAS-NMR. J. Non-Cryst. Solids 127 (1), 53–64.
- Mcmillan, P.F., Poe, B.T., Stanton, T.R., Remmele, R.L., 1993. A Raman-spectroscopic study of H/D isotopically substituted hydrous aluminosilicate glasses. Phys. Chem. Miner. 19 (7), 454–459.
- Mysen, B., 1997. Aluminosilicate melts: Structure, composition and temperature. Contrib. Mineral. Petrol. 127 (1–2), 104–118.
- Mysen, B., 2007a. Partitioning of calcium, magnesium, and transition metals between olivine and melt governed by the structure of the silicate melt at ambient pressure. Am. Mineral. 92 (5–6), 844–862.

- Mysen, B.O., 2007b. The solution behavior of H₂O in peralkaline aluminosilicate melts at high pressure with implications for properties of hydrous melts. Geochim. Cosmochim. Acta 71 (7), 1820–1834.
- Mysen, B., 2013a. Effects of fluid and melt density and structure on high-pressure and high-temperature experimental studies of hydrogen isotope partitioning between coexisting melt and aqueous fluid. Am. Mineral. 98 (10), 1754–1764.
- Mysen, B., 2013b. Hydrogen isotope fractionation between coexisting hydrous melt and silicate-saturated aqueous fluid: an experimental study in situ at high pressure and temperature. Am. Mineral. 98 (2–3), 376–386.
- Mysen, B., Richet, P., 2018. Silicate Glasses and Melts. Elsevier.
- Pineau, F., Shilobreeva, S., Kadik, A., Javoy, M., 1998. Water solubility and D/H fractionation in the system basaltic andesite-H₂O at 1250 °C and between 0.5 and 3 kbars. Chem. Geol. 147 (1–2), 173–184.
- Pope, E.C., Bird, D.K., Rosing, M.T., 2012. Isotope composition and volume of Earth's early oceans. Proc. Natl. Acad. Sci. U. S. A. 109 (12), 4371–4376.
- Richet, P., Bottinga, Y., Javoy, M., 1977. Review of Hydrogen, Carbon, Nitrogen, Oxygen, Sulfur, and Chlorine Stable Isotope Fractionation among Gaseous Molecules. Annu. Rev. Earth Planet. Sci. 5, 65–110.
- Richet, P., Roux, J., Pineau, F., 1986. Hydrogen Isotope Fractionation in the System $\rm H_2O$ liquid NaAlSi $_3O_8$ New Data and comments on D/H Fractionation in Hydrothermal experiments. Earth Planet. Sci. Lett. 78 (1), 115–120.
- Robert, E., Whittington, A., Fayon, F., Pichavant, M., Massiot, D., 2001. Structural characterization of water-bearing silicate and aluminosilicate glasses by highresolution solid-state NMR. Chem. Geol. 174 (1–3), 291–305.
- Saccocia, P.J., Seewald, J.S., Shanks, W.C., 2009. Oxygen and hydrogen isotope fractionation in serpentine-water and talc-water systems from 250 to 450 $^{\circ}$ C, 50 MPa. Geochim. Cosmochim. Acta 73 (22), 6789–6804.

- Schaller, T., Sebald, A., 1995. One-Dimensional and 2-Dimensional ¹H Magic-Angle-Spinning experiments on Hydrous Silicate-Glasses. Solid State Nucl. Magn. Reson. 5 (1), 89–102.
- Shaw, A.M., Hauri, E.H., Fischer, T.P., Hilton, D.R., Kelley, K.A., 2008. Hydrogen isotopes in Mariana arc melt inclusions: Implications for subduction dehydration and the deep-Earth water cycle. Earth Planet. Sci. Lett. 275 (1–2), 138–145.
- Suzuoki, T., Epstein, S., 1976. Hydrogen Isotope Fractionation between OH-Bearing Minerals and Water. Geochim. Cosmochim. Acta 40 (10), 1229–1240.
- Vennemann, T.W., ONeil, J.R., 1996. Hydrogen isotope exchange reactions between hydrous minerals and molecular hydrogen .1. A new approach for the determination of hydrogen isotope fractionation at moderate temperatures. Geochim. Cosmochim. Acta 60 (13), 2437–2451.
- Wang, Y., Cody, S.X., Foustoukos, D., Mysen, B.O., Cody, G.D., 2015. Very large differences in intramolecular D-H partitioning in hydrated silicate melts synthesized at upper mantle pressures and temperatures. Am. Mineral. 100 (5–6), 1182–1189.
- Xue, X.Y., Kanzaki, M., 2001. Ab initio calculation of the ¹⁷O and ¹H NMR parameters for various OH groups: Implications to the speciation and dynamics of dissolved water in silicate glasses. J. Phys. Chem. B 105 (17), 3422–3434.
- Xue, X.Y., Kanzaki, M., 2004. Dissolution mechanisms of water in depolymerized silicate melts: Constraints from ¹H and ²⁹Si NMR spectroscopy and ab initio calculations. Geochim. Cosmochim. Acta 68 (24), 5027–5057.
- Zarei, A., Klumbach, S., Keppler, H., 2018. The Relative Raman Scattering Cross Sections of H₂O and D₂O, with Implications for in Situ Studies of Isotope Fractionation. Acs Earth and Space Chemistry 2 (9), 925–934.
- Zotov, N., Keppler, H., 1998. The influence of water on the structure of hydrous sodium tetrasilicate glasses. Am. Mineral. 83 (7–8), 823–834.